Journal of Materials Science: Materials in Medicine (2019) 30:26
https://doi.org/10.1007/s10856-019-6227-9

TISSUE ENGINEERING CONSTRUCTS AND CELL SUBSTRATES

Original Research

Osseointegration of titanium scaffolds manufactured by selective laser melting in rabbit femur defect model

Aranka Ilea[1] · Oana-Gabriela Vrabie[2] · Anida-Maria Băbțan[1] · Viorel Miclăuş[3] · Flavia Ruxanda[3] · Melinda Sárközi[4] · Lucian Barbu-Tudoran[5,6] · Voicu Mager[7] · Cristian Berce[8] · Bianca Adina Boşca[9] · Nausica Bianca Petrescu[1] · Oana Cadar[10] · Radu Septimiu Câmpian[1] · Réka Barabás[4]

Received: 21 September 2018 / Accepted: 28 January 2019 / Published online: 12 February 2019

Abstract

The aim of this study was to assess the osseointegration of two series of titanium (Ti) scaffolds with 0.8 and 1 mm cell size obtained by Selective Laser Melting (SLM) technique. One of the series had the Ti surface unmodified, while the other had the Ti surface coated with silicon-substituted nano-hydroxyapatite (nano-HapSi). The scaffolds were implanted in the femur bone defects of 6 White Californian male rabbits: three animals were implanted with 0.8 mm cell size scaffolds and three animals with 1 mm cell size scaffolds, respectively. The bone fragments and scaffolds harvested at 2, 4 and 6 months were histologically analyzed using conventional light microscopy (LM) and scanning electron microscopy (SEM) for the qualitative evaluation of the bone tissue formed in contact with the scaffold. Both LM and SEM images indicated a better osseointegration for nano-HapSi coated Ti scaffolds. LM revealed that the compact bone formed in the proximity of nano-HapSi-coated scaffolds was better organized than spongy bone associated with unmodified scaffolds. Moreover, Ti scaffolds with meshes of 0.8 mm showed higher osseointegration compared with 1 mm. SEM images at 6 months revealed that the bone developed not only in contact with the scaffolds, but also proliferated inside the meshes. Nano-HapSi-coated Ti implants with 0.8 mm meshes were completely covered and filled with new bone. Ti scaffolds osseointegration depended on the mesh size and the surface properties. Due to the biocompatibility and favorable osseointegration in bone defects, nano-HapSi-coated Ti scaffolds could be useful for anatomical reconstructions.

These authors contributed equally: Aranka Ilea, Oana-Gabriela Vrabie and Anida-Maria Băbțan

✉ Bianca Adina Boşca
biancabosca@yahoo.com

[1] Department of Oral Rehabilitation, Oral Health and Dental Office Management, Faculty of Dentistry, "Iuliu Haţieganu" University of Medicine and Pharmacy, Cluj-Napoca, Victor Babeş Str., no 15, Cluj-Napoca, Romania

[2] Faculty of Dentistry, "Iuliu Haţieganu" University of Medicine and Pharmacy, Cluj-Napoca, Victor Babeş Str., no 8, Cluj-Napoca, Romania

[3] Department of Histology and Embriology, Faculty of Veterinary Medicine, University of Agricultural Sciences and Veterinary Medicine Cluj-Napoca, Mănăştur Avenue, no 3-5, Cluj-Napoca, Romania

[4] Department of Chemistry and Chemical Engineering, Faculty of Chemistry and Chemical Engineering, Hungarian Line of Study, "Babeş Bolyai" University Cluj-Napoca, Arany Janos Str., no 11, Cluj-Napoca, Romania

[5] Department of Molecular Biology and Biotechnology, Faculty of Biology, "Babeş Bolyai" University Cluj-Napoca, Republicii (Gheorghe Bilaşcu) Str., no 44, Cluj-Napoca, Romania

[6] National Institute for Research and Development of Isotopic and Molecular Technologies, Cluj-Napoca, Donat Str., no 67-103, Cluj-Napoca, Romania

[7] Postdoctorand of Technical University of Cluj-Napoca, Muncii Avenue, no103-105, Cluj-Napoca, Romania

[8] Biobase Department of "Iuliu Haţieganu" University of Medicine and Pharmacy Cluj-Napoca, Louis Pasteur Str., no 6, Cluj-Napoca, Romania

[9] Department of Histology, Faculty of Medicine, "Iuliu Haţieganu" University of Medicine and Pharmacy Cluj-Napoca, Louis Pasteur Str., no 4, Cluj-Napoca, Romania

[10] INCDO-INOE 2000, Research Institute for Analytical Instrumentation, Cluj-Napoca, Donath Str., no 67, Cluj-Napoca, Romania

Graphical Abstract

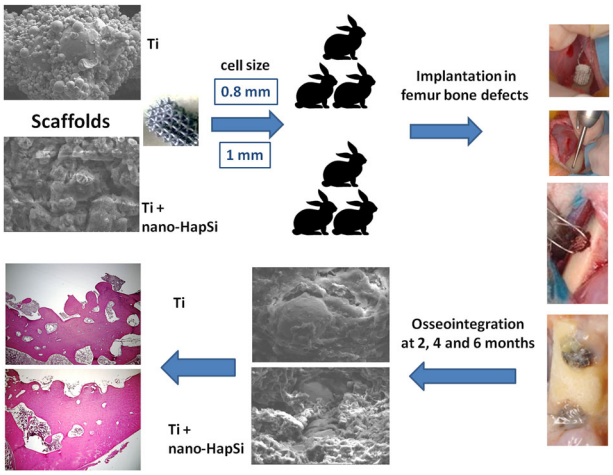

1 Introduction

There are increasing demands for metal implants that could shorten the therapeutic and hospitalization periods and increase the treatment success rate for patients with poor bone quality. Metal implants such as 316 L stainless steel, cobalt–chromium (Co–Cr) alloys and titanium (Ti) based materials have the greatest potential for long-term orthopedic and dental applications due to their good mechanical properties and resilience compared to alternative biomaterials (polymers, ceramics) [1]. Particularly, Ti offers good biocompatibility and excellent mechanical properties [2–4]. Despite the successful outcomes, the surface activation of Ti implants is a key factor for rapid and stable bone tissue integration [5, 6]. The surface treatments (superficial conditioning with different compounds, mechanical treatments, anodic oxidation [7], chemical or mechanical etching [5, 8], application of simvastatin [9] and coating with various materials (hydroxyapatite (Hap), titanium oxide [9–11]), promote bone regeneration and improve implant osseointegration.

In vitro observations of cells development on the Ti reconstructions with nanostructures coating show promising results [12–15]. Some in vivo studies concluded that the integration of the nanostructures coated implants had a better osseointegration than the uncoated ones [12, 15]. A problem that occurred in some cases seemed to be the method by which the nanostructures were applied on the surface of the Ti reconstructions. On the other hand, there also were some studies that did not find a significant difference between the coated implants and the controls [11, 16]. However, some modifications may diminish the mechanical properties, resulting in surface micro-cracks and increased corrosion rates, which may affect the surrounding cells and tissues. Consequently, the biocompatibility of orthopedic or dental metallic implants could be significantly enhanced using bioceramics as coating materials. Synthetic nano-Hap mimics the composition of natural bone due to biocompatibility, low cytotoxicity and appropriate mechanical properties [17, 18].

Several conventional methods for obtaining solid and porous Ti based materials were described, including: casting, space holder technology, foaming and powder metallurgy; but these methods are time, material and energy consuming [19]. Recently, advanced technologies such as selective laser melting (SLM) and additive manufacturing allows the design and manufacturing of complex shape parts in a simple, fast and efficient way [4, 8].

The literature data on the influence of Ti scaffolds pore size on the osseointegration process are controversial. The in vitro studies on human osteoblasts showed that cells migration into the pores of nickel-titanium (Ni-Ti) alloy scaffolds were better in small sized-pores (277.2 and 337.6 μm) than in larger pores (566.5 μm) [20]. Similarly, the studies on human osteoblasts with smaller pores (400–620 μm and pyramidal scaffolds design) exhibited the highest metabolic activity and ingrowth compared to higher pores (700 × 700 μm and cubic scaffolds design and 400–1000 μm and diagonal scaffolds design) [21]. Contrary, an in vivo study showed that higher pore size and higher Ti scaffolds porosity had positive effects on the amount of new bone growth evaluated by histomorphometric examination, although most of the smaller pores (180 μm) were more fulfilled than the larger ones (300 μm) [22]. Although the optimum matrix size required for osseointegration was reported as 150–600 μm, our study goal was to exceed this upper limit in order to figure out if slight increase of pores size assures a good bone integration of the scaffolds and if

the pattern of osseointegration process are maintained (the scaffolds with smaller pores have better bone integration than the bigger ones). So, the aim of this study was to assess the osseointegration of 2 series of Ti scaffolds with 0.8 and 1 mm meshes, with unmodified and modified surfaces, obtained by selective laser melting technique.

2 Materials and methods

2.1 Preparation of unmodified and surface-modified Ti scaffolds

The Ti matrices were produced by SLM process using MCP ReaLizer II SLM 250 (SLM Solutions Holding GmbH, Lübeck, Germany). The discs of 5 mm diameter and the cell size unit of 0.8 and 1 mm were manufactured with 75 W laser power, 10 µm point distance and 60 µs exposure time. The porosity of scaffolds, calculated based on the relationship between the density of samples and the standard bulk material, was of 76.4% for scaffolds with 0.8 mm cells size unit and 84.5% for scaffolds with 1 mm cells size unit. After the removal from the manufacturing platform, the specimens were cleaned of the remaining powder by blowing compressed air and then by immersion into distilled water for 10 min in a Fritsch Laborette 17 ultrasonic bath (Fritsch GmbH, Idar-Oberstein, Germany). Before implantation, the scaffolds were sterilized at 134 °C, for 35 min, using an MELAG-Vacuklav 24B + autoclave (MELAG, Berlin, Germany).

Half of Ti scaffolds were superficially-coated with silicon-substituted nano-hydroxyapatite (nano-HapSi) (10 wt.% Si) prepared by a precipitation method [18] as follows: the scaffolds were immersed in a nano-HapSi/water suspension (10 g/L) for 15 min and dried for 3 h, at 105 °C; this procedure was repeated 3 times. The resulted scaffolds were dried for 1 h at 450 °C.

2.2 Animals

The study was approved by the Ethics Committee of "Iuliu Haţieganu" University of Medicine and Pharmacy Cluj-Napoca, no.165/20.04.2016 and was conducted at the Animal Facility Laboratory. All applicable institutional and national guidelines for the care and use of animals were followed.

Six White Californian male rabbits were used for this preliminary study. All the procedures performed on the laboratory animals were according to the rules and regulations of the European Community in as far as the care and use of lab animals (63/2010) and the Romanian Law 43/2014 regarding the protection of animals used in scientific purposes. During the study optimal living conditions for the subjects were insured, adapted to their natural living environment. The animals were habited in cages according to the regulations specified in the legislation with enough space for the daily movement, optimal temperature and humidity conditions (standard temperature 20–24 °C, humidity 50 ± 20%). The subjects had free access to water and their diet consisted of granulated fodder, greens and hay. The artificial lighting provided a cycle of 12 h of light and 12 h of darkness.

2.3 Procedure and data collection

The rabbits received Ti implants with the cell size of 0.8 mm ($n = 3$) and 1 mm ($n = 3$), respectively. For each subject, two circular bone defects in the proximal third of the left femur were performed at a distance of 5–6 mm from each other. To minimize the number of animals included in the study, for each rabbit, two implants were placed in the femur bone (one implant with unmodified Ti scaffolds and one implant with surface-modified Ti scaffolds). Of the six rabbits, three received scaffolds with cell size of 0.8 mm and three with cells size of 1 mm.

General anesthesia was induced by administering an intramuscular injection of ketamine (0.5 ml/kg) and xylazine hydrochloride (0.25 ml/kg). Under aseptic conditions, a 2 cm longitudinal skin incision was performed on the proximal third of the leg. The femur bone surface was exposed by dilating the muscular fascia between the biceps and the femoral quadriceps and the periosteum was removed. With a sterile syringe needle, the outline of the matrix was plotted on the bone surface and then under continuous cooling, a circular bone defect was performed using a globular drill. The matrices were inserted into the bone defect and fixed by cerclage. Ni-Ti orthodontic wire (Denxy Ortho, Hunan, China) with a diameter of 0.3 mm and round profile was used to make the cerclage. The wire was inserted through the first row of mesh scaffold and fixed it by twisting. The bone defects were not covered with any material, the scaffolds being covered by the periosteum. The surgical wound was sutured in two layers. Postoperatively, non steroidal anti-inflammatory drugs (0.2 mg Meloxicam/kg body weight/24 h by intramuscular injection for 5 days) and antibiotics (1.8 ml Enrofloxacin/24 h by subcutaneous injection for 5 days) were administered to prevent infection and to control pain. After the surgical procedures, the rabbits were confined to cages and maintained with a regular laboratory diet. Wound healing and recovery of limb mobility were noticed and each animal was kept in individual cage in order to avoid unwanted accidents.

The bone fragments and scaffolds were harvested at 2, 4 and 6 months. The rabbits were euthanized, under general anesthesia, by intracardiac injection, using a saturated potassium chlorine solution. Bone fragments containing implanted matrices were harvested with 5 mm of safety margins.

2.4 Light microscopy and scanning electronic microscopy (SEM)/Energy Dispersive X-Ray (EDX)

The specimens were numbered and decalcified. The Ti matrices were removed and SEM/EDX analysis was performed using a Hitachi SU8230 (Tokyo, Japan) microscope. The electron microscope was coupled with an Aztec X-Max 1160 EDX detector (Oxford Instruments). The surrounding bone tissue was embedded in paraffin, sectioned, stained and conventional histological examination was performed with an Olympus BX41(Tokyo, Japan) microscope using Goldner's trichromic and hematoxylin-eosin stain.

3 Results

3.1 Light microscopy

3.1.1 Bone repair at 2 months after implantation

After 2 months, at the intervention site, healing of the bone defect occurred by endochondral ossification (Fig. 1). A zone of hyaline cartilage was formed at the interface with the implant (Fig. 1a); this is an early stage of bone healing. The hyaline cartilage contained numerous enlarged chondrocytes embedded into the cartilage matrix and organized in isogenous groups (Fig. 1b). In the adjacent zone, more advanced ossification could be seen; trabeculae consisted of calcified cartilage matrix in the central part and bone tissue: bone matrix, ostocytes in lacunae and osteoblasts on the surface (Fig. 1a). The profound zones contained woven, primary bone: thin bone trabeculae and large intercommunicating areoles with bone marrow and numerous blood vessels. The woven bone had non-lamellar structure and disorganized architecture. Bone trabeculae contained large ovoid osteocytes and bone matrix with low mineral content; on the surface of the bone trabeculae, active osteoblasts and osteoclasts were involved in intense bone remodeling (Fig. 1b).

3.1.2 Bone repair at 4 months after implantation

After 4 months, the bone healing at the intervention site was complete; the newly formed bone tissue was secondary, mature bone with a lamellar structure Moreover, at the interface with the implant, the tissue specimens exhibited an indented surface, which suggests that the bone tissue proliferated into the pores of the scaffold, which was a sign of efficient osseointegration. (Figs 2 and 3). However, depending on the composition of Ti scaffolds, the bone tissue exhibited different morphology and architecture.

At the implantation site of unmodified surface Ti scaffolds, spongy, cancellous bone was formed (Fig. 2). Bone trabeculae were thick and consisted of bone lamellae with a random orientation (Fig. 2a). Within trabeculae, resting osteocytes were smaller and flattened, embedded into the calcified matrix. On the surface, both active and resting osteoblasts could be identified, but fewer osteoclasts, hence the limited bone remodeling (Fig. 2b). The medullary component represented by the areoles with bone marrow occupied an important volume in the bone tissue (Fig. 2a). Upon the detachment of the bone specimen from the implant, fragments of bone tissue were fractured, because the spongy bone associated with the Ti scaffolds had a low resistance (Fig. 2a).

The bone tissue associated with Ti scaffolds coated with nano-HapSi was dense, compact bone with a cylindrical-lamellar architecture (Fig. 3). Bone lamellae were organized in concentric arrays surrounding Haversian canals and formed osteons (Fig. 3a). Within lamellae, formative osteocytes were larger and the lacunae were surrounded by osteoid (Fig. 3b). The medullary component, represented by the Haversian canals was reduced compared with the volume of the bone tissue, which was predominant.

The compact bone formed in the proximity of the Ti + nano-HapSi scaffolds protruded into the pores of the scaffold but upon implant removal the tissue was not fractured, suggesting a more resistant tissue structure (Fig. 3a).

In the diaphysis of the long bone, where the implants were inserted, compact haversian bone is normally present. Therefore, the repair process was more efficient for the Ti scaffolds coated by nano-HapSi, which induced the formation of the haversian bone, compared with the scaffolds without nano-HapSi, which induced the formation of cancelous bone.

3.2 SEM/EDX analysis

The SEM images revealed the initial aspect of unmodified surfaces of Ti scaffolds (Ti merged particles) and surface-modified Ti scaffolds (Ti and nano-HapSi particles formed at the surface of the scaffold) (Fig. 4).

Figure 5 shows the chemical composition of 0.8 mm unmodified Ti scaffolds (calcium (Ca), Ti, oxygen (O)—Fig. 5a) and 0.8 mm surface-modified Ti scaffolds (Ti, carbon (C), Ca, O and phosphorus (P)—Fig. 5b) before implantation.

3.2.1 Biocompatibility of the Ti scaffolds at 4 months after implantation

The SEM images of scaffolds 4 months after implantation revealed the initial attachment and cell proliferation on the surface matrix (Fig. 6). The surface properties and the cell size played an important role in modulating the cellular behavior. On the unmodified Ti surfaces, the fibroblast-like

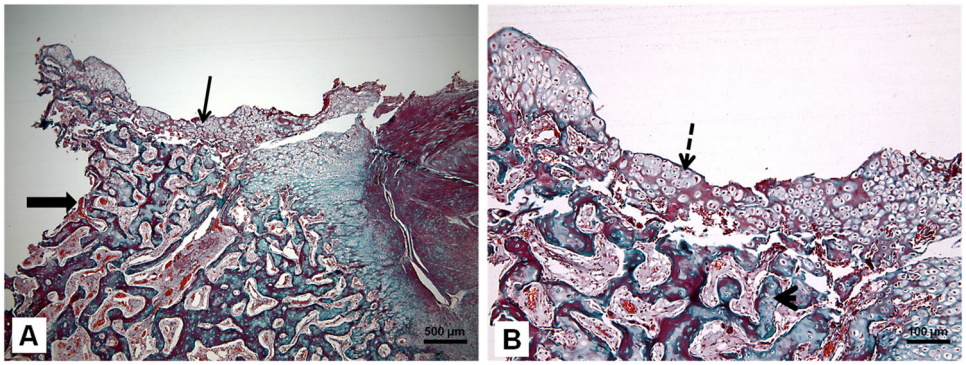

Fig. 1 Photomicrograph of the intervention site after 2 months. Tissue harvested by detachment from the Ti scaffold with unmodified surface and 1 mm cells size; **a** hyaline cartilage formed at the interface with the implant (*thin arrow*) and woven bone in the profound zone (*thick arrow*); **b** the hyaline cartilage with enlarged chondrocytes in lacunae (*dotted arrow*) and thin bone trabeculae delimiting intercommunicating areoles (*arrowhead*); Goldner's trichromic stain

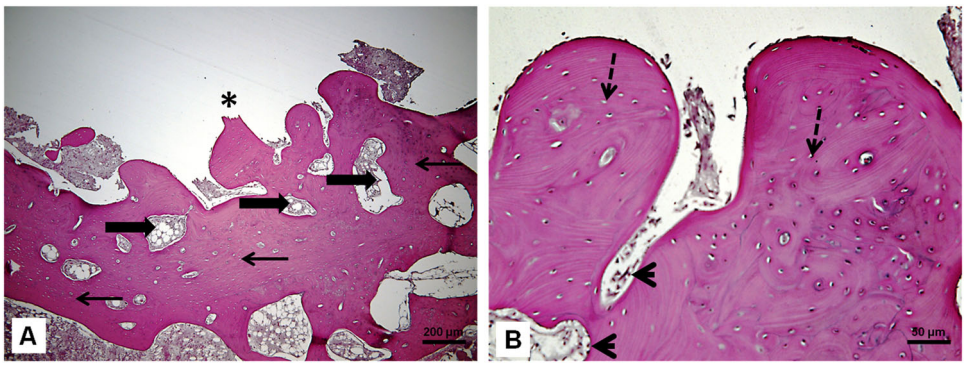

Fig. 2 Photomicrograph at the implantation site of Ti scaffolds after 2 months. Tissue harvested by detachment from the Ti scaffold with unmodified surface and 0.8 mm cells size; **a** cancelous bone containing thick trabeculae (*thin arrows*) and areoles with bone marrow (thick arrows); rupture of the bone tissue proliferated into the pores of the scaffold (*asterisk*); **b** resting osteocytes in lacunae (dotted arrows) and osteoblasts on the surface of the bone trabeculae (*arrowheads*); Hematoxylin and eosin stain

cells proliferated between the indentations of the Ti particles (Fig. 6a–d, i–l), whereas on the coated nano-HapSi Ti scaffolds, the cells completely covered the surface and extended cytoplasmic processes in close relationship with Hap crystals (Fig. 6e–h, m–p). Additionally, the scaffolds with pores of 0.8 mm seemed to provide more support for the cells developing on their surface (Fig. 6i–p).

3.2.2 Biocompatibility of the Ti scaffolds at 6 months after implantation

The SEM images of scaffolds 6 months after implantation revealed fibroblast-like cells showing an intense proliferation and attachment not only on the scaffolds surface, but also inside the pores. Moreover, the extracellular matrix was also secreted, enclosing the cells and filling in the spaces inside the scaffolds (Fig. 7). The attachment and spreading characteristics also varied according to the surface. The tissue formed in the pores of the Ti scaffolds exhibited a loose arrangement of the cells and fibers. The cells that developed on the nano-HapSi coated Ti scaffolds showed an extensive spreading, the fibers were more numerous and the tissue was more condensed inside the pores (Fig. 7e–h, m–p), mainly in the 0.8 mm pores (Fig. 7m–p).

In the case of scaffolds 6 months implantation (Fig. 8), beside Ti, C, Ca, O and P, the presence of nitrogen (N) and sulfur (S) was also observed, indicating the formation of biomolecules [23].

4 Discussion

Bone is a specialized connective tissue capable to regenerate and to restore its architectural integrity after injuries. But, when the bone defect exceeds the critical size, the stability of the new bone is affected. Ti scaffolds provide mechanical strength in order to maintain a stable support and to enable the loads transmission. Ti implant fixation with new bone formation involves a cascade of cellular and extracellular biological events and a minimum of 6 weeks to

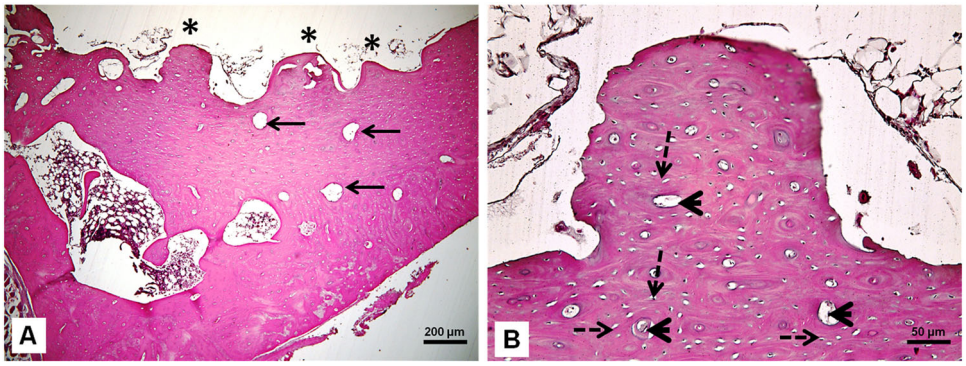

Fig. 3 Photomicrograph at the implantation site of Ti + nano-HapSi scaffolds after 4 months. Tissue harvested by detachment from the Ti + nano-HapSi scaffold with unmodified surface and 0.8 mm cells size; **a** compact bone containing osteons (*thin arrows*); the bone tissue protrusions into the pores of the scaffold, without signs of rupture (*asterisk*); **b** formative osteocytes in lacunae (*dotted arrows*) in concentric lamellae surrounding the Haversian canals (*arrowheads*); hematoxylin and eosin stain

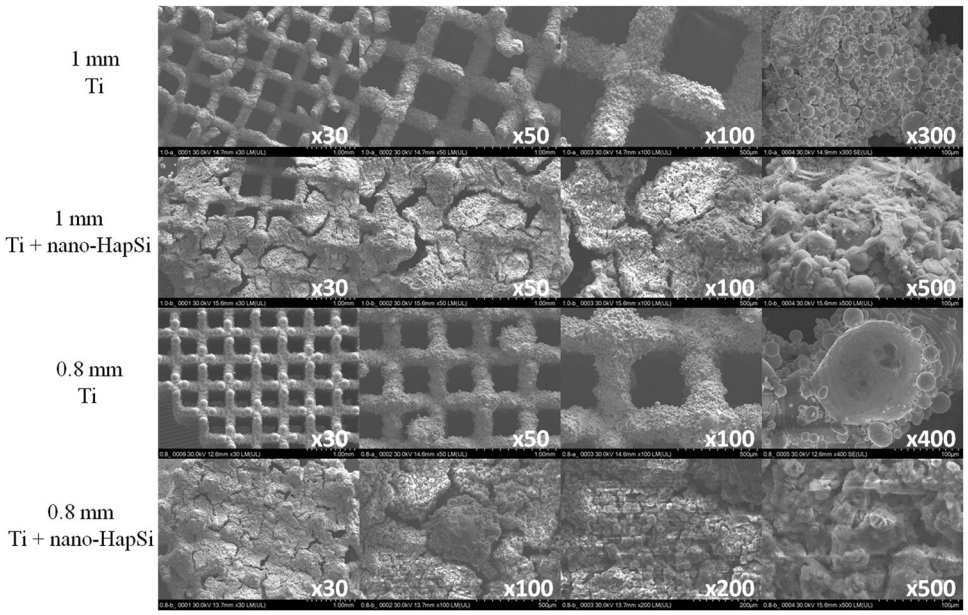

Fig. 4 SEM images of the scaffolds before implantation

3 months is required for clinical healing [3]. Ti is a biocompatible material and promotes bone regeneration because it does not inhibit cell proliferation and has osteoconductive properties [24]. Furthermore, the materials associated with Ti or the surface conditioning of the scaffolds could enhance the bone regenerative potential. Xie et al. tested the Ti fiber reinforced composites associated with autologous bone particles and reported an improved osteogenic performance due to the osteocytes present in the implants [25]. On the other hand, Antonov et al. demonstrated that porous coated Ti implants stimulated the proliferation and the osteogenic differentiation of the mesenchymal stem cells; the autologous osteoprogenitor cells loaded onto porous Ti implants could stimulate the bone healing around the implant and the osseointegration [26]. This may be an alternative to the autologous and allogenic bone grafts. Yoo et al. proposed bioactive Ti implants obtained by the conjugation of a synthetic peptide similar to the bone morphogenetic protein-2 to the surface of a Ti alloy. Their results indicated that the peptide-conjugated surfaces enhanced the rate of bone growth, mainly in the initial phase of bone healing [3]. However, obtaining autologous mesenchymal stem cells for loading the implants is laborious; therefore the use of biochemical modifications of the Ti surfaces. The results of our preliminary study were consistent with other studies that reported a good integration of the implants with the surface enriched with Ca ions, such as the nanostructured Ca-incorporated implants placed in the human jaw bones. Mangano et al. examined the interface between the human bone tissue and the nanostructured calcium-incorporated surface of an implant placed in the posterior maxilla, after

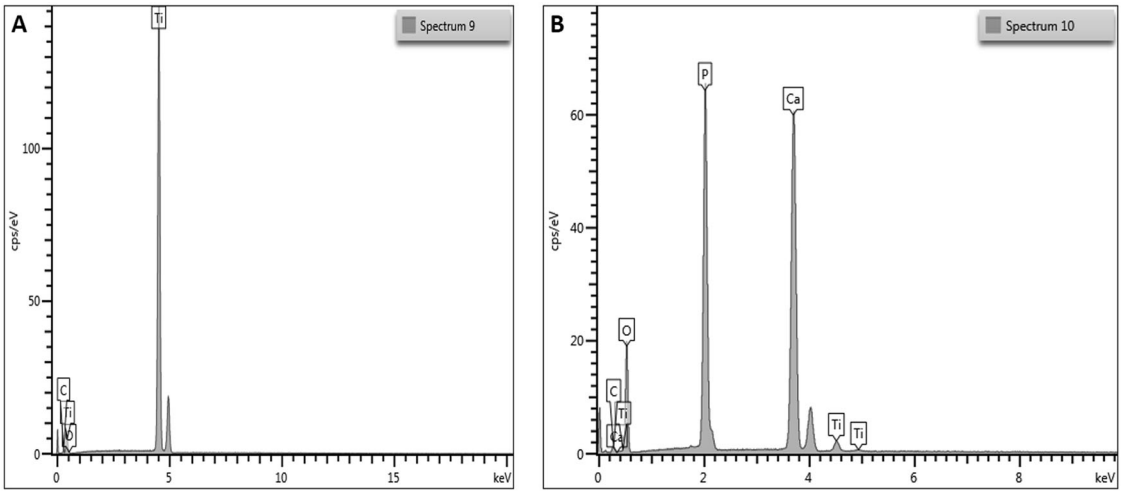

Fig. 5 EDX spectra before implantation. **a** 0.8 mm unmodified Ti scaffolds and **b** 0.8 mm surface-modified Ti scaffolds

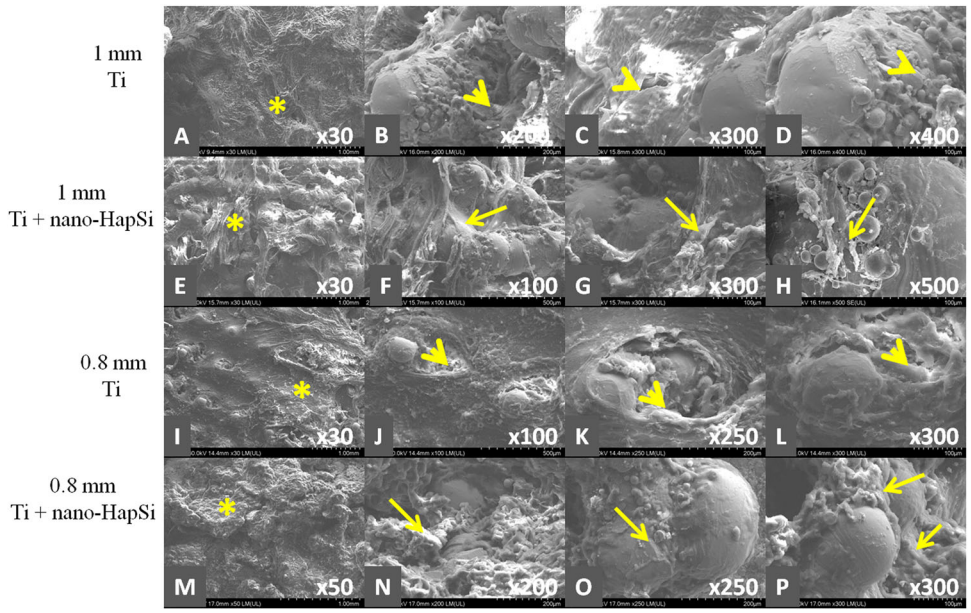

Fig. 6 SEM images of the scaffolds 4 months after implantation. **a**, **e**, **i**, **m** scaffolds surfaces partially covered by fibroblast-like cells (*asterisks*); **b–d**, **j–l** cells proliferating between the Ti particles (*arrowheads*); **f–h**, **n–p** flattened cells with cytoplasmic processes attached to the scaffolds surfaces (*thin arrows*)

the traumatic mobilization of the implant. After 1 month, the surface was completely covered by trabecular bone firmly anchored to the implant [27].

The implants' surface topography and texture also influence the bone repair. The rough Ti surfaces seem to be more beneficial materials for osseointegration, especially during the early phases of bone healing, when the cell attachment and proliferation is critical [28]. These findings are consistent with our results since the implants conditioned with Hap, which had a rougher surface compared with the untreated implants enabled a better osseointegration. Porous implant structures are more advantageous compared with bulk implants, because they promote the proper interaction between the bone and the implant and strengthen the bone-implant interface [29–31]. The pores in the Ti scaffolds are better integrated, since the native bone has a porous structure, with different porosity in compact and in spongy bone respectively [32]. In our study, the bone tissue proliferated in the pores of the Ti scaffolds optimizing the anchoring of the surrounding bone and increasing the implant's stability.

The purpose of our study was to find out whether the size of Ti scaffolds pores made with high precision by SLM technique could influence the osseointegration process. Moreover, the role of nano-HapSi coating of Ti scaffolds surfaces on the new bone formation was assessed. The newly formed bone tissue associated with nano-HapSi coated Ti scaffolds had a more organized architecture and higher resistance, which are characteristic for the haversian bone; moreover, the bone tissue exhibited advanced and intense bone remodeling compared with unmodified Ti scaffolds.

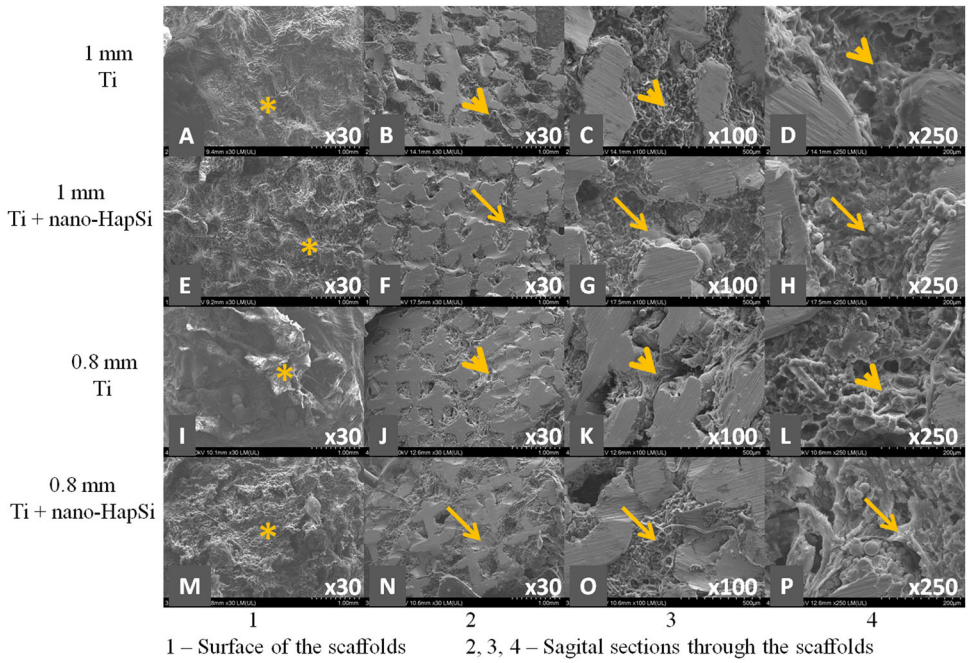

Fig. 7 SEM images of the scaffolds at 6 months after implantation. **a**, **e**, **i**, **m** scaffolds surfaces completely covered by cells and extracellular matrix (*asterisks*); **b–d**, **j–l** tissue proliferating inside the scaffolds, without filling the entire pores (*arrowheads*); **f–h**, **n–p** densely packed fibroblast-like cells and fibers firmly attached to the surfaces (*thin arrows*)

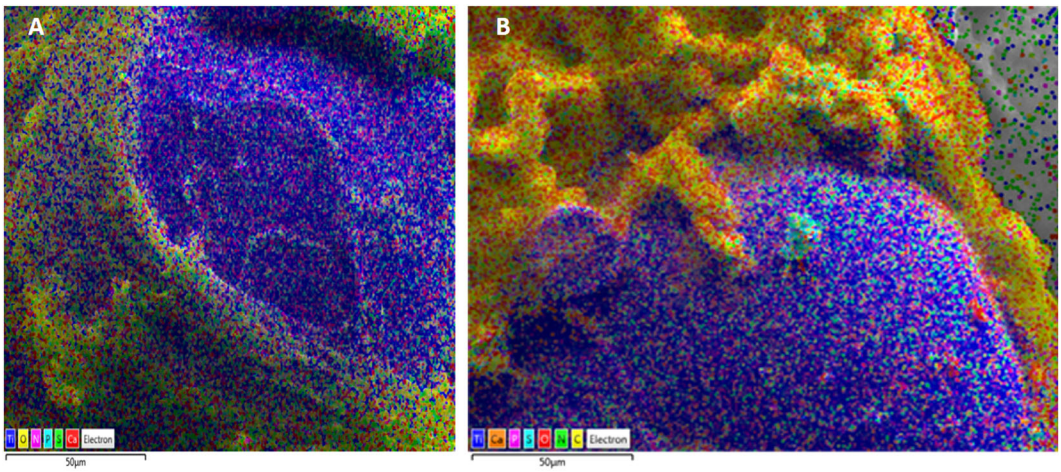

Fig. 8 Elemental distribution map of the scaffolds at 6 months after implantation. **a** 0.8 mm unmodified Ti scaffolds and **b** 0.8 mm surface-modified Ti scaffolds

These findings suggest that the presence of nano-HapSi at the interface between the scaffold and the bone tissue sustained the new bone formation and promoted the repair processes of the bone defect. The SEM images revealed a better developed bone at the interface with the Ti + nano-HapSi compared with unmodified Ti implants, suggesting that Ca ions from nano-HapSi had a beneficial effect on osseointegration.

Additionally, the new bone tissue proliferated inside the scaffold had a more condensed aspect due to increased spanning and bridging for meshes of 0.8 mm. The explanation could be that scaffolds with 0.8 mm meshes size had higher surface area for the same volume; moreover, the Ti + nano-HapSi scaffolds had a rougher surface, which promoted the attachment and development of the osteoprogenitor cells and provided increased support for the bone matrix.

The study limitations were the small number of animals and analyzed specimens and also the difficulties in obtaining more data by sequential examinations at different time points. Further studies are required in order to validate the results on larger numbers of laboratory animals so that the osseointegration process would be assessed sequentially (through several types of examinations and quantification of the results). Additionally, a larger number of scaffolds with variable cell size are needed for assessing the upper and

lower limits of mesh sizes that provide optimal osseointegration (or the best osseointegration) without significantly altering the physical properties of the implanted scaffold. Furthermore, the limits of compromise between the osseointegration process and the physical properties of the implanted material should be determined.

5 Conclusions

Our preliminary study indicated that the Ti scaffolds manufactured by SLM were well osseointegrated in vivo. The nano-HapSi coating on the scaffold surface and the small size of the meshes promoted the new bone formation and improved the osseointegration process. The integration of the implants was gradual, with an increased bone proliferation on the surface and inside the scaffolds meshes at 6 months after implantation. The obtained results in the animal model for studying the osteointegration processes of the Ti matrix (modified or unmodified surfaces) made by the SLM are prerequisites for studying the osseointegration on human cohorts. Thus, personalized medicine desideratum can be achieved, so that bone grafting can be accomplished with a custom implant for each patient.

Acknowledgements This study was funded by the internal grant No 4995/20/08.03.2016 within the "Iuliu Haţieganu" University of Medicine and Pharmacy, Cluj-Napoca, Romania and partially by PhD Grant of "Iuliu Haţieganu" University of Medicine and Pharmacy Cluj-Napoca, No 3999/01.10.2016.

Compliance with ethical standards

Conflicts of interest The authors declare no conflicts of interest with respect to the authorship and/or publication of this article.

References

1. Li JP, Habibovica P, van del Doel M, Wilson CE, de Wijn JR, van Blitterswijk CA et al. Bone ingrowth in porous titanium implants produced by 3D fiber deposition. Biomaterials. 2007;28:2810–2820.
2. Ozcan M, Hammerle C. Titanium as a reconstruction and implant material in dentistry: advantages and pitfalls. Mater (Basel). 2012;5:1528–1545.
3. Yoo JJ, Park YJ, Rhee SH, Chun HJ, Kim HJ. Synthetic peptide-conjugated titanium alloy for enhanced bone formation in vivo. Connect Tissue Res. 2012;53:359–365.
4. Taniguchi N, Fujibayashi S, Takemoto M, Sasaki K, Otsuki B, Nakamura T et al. Effect of pore size on bone ingrowth into porous titanium implants fabricated by additive manufacturing: an in vivo experiment. Mater Sci Eng C Mater Biol Appl. 2016;59:690–701.
5. Salou L, Hoornaert A, Louarn G, Layrolle P. Enhanced osseointegration of titanium implants with nanostructured surfaces: an experimental study in rabbits. Acta Biomater. 2015;11:494–502.
6. Wieding J, Lindner T, Bergschmidt P, Bader R. Biomechanical stability of novel mechanically adapted open-porous titanium scaffolds in metatarsal bone defects of sheep. Biomaterials. 2015;46:35–47.
7. Ban J, Kang S, Kim J, Lee K, Hyunpil L, Vang M et al. MicroCT analysis of micro-nano titanium implant surface on the osseointegration. J Nanosci Nanotechnol. 2015;15:172–175.
8. Deppe H, Grunberg C, Thomas M, Sculean A, Benner KU, Bauer FJ. Surface morphology analysis of dental implants following insertion into bone using scanning electron microscopy: a pilot study. Clin Oral Implants Res. 2015;26:1261–1266.
9. Yong-Dae K, Yang DH, Lee DW. A titanium surface-modified with nano-sized hydroxyapatite and simvastatin enhances bone formation and osseointegration. J Biomed Nanotechnol. 2015;11:1007–1015.
10. Horasawa N, Yamashita T, Uehara S, Udagawa N. High-performance scaffolds on titanium surfaces: osteoblast differentiation and mineralization promoted by a globular fibrinogen layer through cell-autonomous BMP signaling. Mater Sci Eng C Mater Biol Appl. 2015;46:86–96.
11. Svanborg LM, Meirelles L, Stenport VF, Kjellin P, Currie F, Andersson M et al. A Evaluation of bone healing on sandblasted and acid etched implants coated with nanocrystalline hydroxyapatite: an in vivo study in rabbit femur. Int J Dent Article. 2014;197581:1–7. https://doi.org/10.1155/2014/197581.
12. Hirota M, Shima T, Sato I, Ozawa T, Iwai T, Ametani A et al. Development of a biointegrated mandibular reconstruction device consisting of bone compatible titanium fiber mesh scaffold. Biomaterials. 2016;75:223–236.
13. Garcia-Gareta E, Hua J, Blunn GW. Osseointegration of acellular and cellularized osteoconductive scaffolds: is tissue engineering using mesenchymal stem cells necessary for implant fixation? J Biomed Mater Res A. 2014;103:1067–1076.
14. Sivolella S, Brunello G, Ferroni L, Berengo M, Meneghello R, Savio G et al. A novel in vitro technique for assessing dental implant osseointegration. Tissue Eng Part C Methods, 2015; https://doi.org/10.1089/ten.TEC.2015.0158.
15. Hirota M, Hayakawa T, Shima T, Ametani A, Tohnai I. High porous titanium scaffolds showed higher compatibility than lower porous beta-tricalcium phosphate scaffolds for regulating human osteoblast and osteoclast differentiation. Mat Sci Eng C Matter. 2015;49:623–631.
16. Yan C, Hao L, Hussein A, Young P. Ti–6Al–4V triply periodic minimal surface structures for bone implants fabricated via selective laser melting. J Mech Behav Biomed. 2015;51:61–73.
17. Sirin HT, Vargel I, Kutsal T, Korkusuz P, Piskin E. Ti implants with nanostructured and HA-coated surfaces for improved osseointegration. Artif Cells Nanomed Biotechnol. 2016;44:1023–1030.
18. Dancu AC, Barabas R, Bogya ES. Adsorption of nicotinic acid on the surface of nanosized hydroxyapatite and structurally modified hydroxyapatite. Cent Eur J Chem. 2011;9:660–669.
19. Zhang LC, Attar H, Calin M, Eckert J. Review on manufacture by selective laser melting and properties of titanium based materials for biomedical applications. Mater Technol. 2016;31:66–76.
20. Jian YT, Yang Y, Tian T, Stanford C, Zhang XP, Zhao K. Effect of pore size and porosity on the biomedical properties and compatibility of porous NiTi alloys. PloS ONE. 2015;10:e0128138.
21. Markhoff J, Wieding J, Weissmann V. Influence of different three-dimensional open porous titanium scaffold designs on human osteoblasts behavior in static and dynamic cell investigations. Mater (Basel). 2015;8:5490–5507.

22. Vasconcellos LM, Leite DO, Oliveira FN, Carvalho YR, Cairo CA. Evaluation of bone ingrowth into porous titanium implant: histomorphometric analysis in rabbits. Braz Oral Res. 2010;24:399–405.
23. Schätzle M, Zinelis S, Markic G, Eliades G, Eliade T. Structural, morphological, compositional, and mechanical changes of palatal implants after use: a retrieval analysis. Eur J Orthod. 2017;39:579–585.
24. Le Guehennec L, Lopez-Heredia MA, Enkel B, Weiss P, Amourig Y, Layrolle P. Osteoblastic cell behaviour on different titanium implant surfaces. Acta Biomater. 2008;4:535–543.
25. Xie H, Ji Y, Tian Q, Wang X, Zhang N, Zhang Y et al. Autogenous bone particle/titanium fiber composites for bone regeneration in a rabbit radius critical-size defect model. Connect Tissue Res. 2017;58:553–561.
26. Antonov B, Bochev I, Mourdjeva M, Kinov P, Tzvetanoc L, Sheitanov I et al. Porous coated titanium implants do not inhibit mesenchimal stem cells proliferation and osteogenic differentiation. Biotechnol Biotec Eq. 2014;27:4290–4293.
27. Yoo JJ, Park YJ, Rhee SH, Chun HJ, Kim HJ. Scanning electron microscope (SEM) evaluation of the interface between a nanostructured calcium-incorporated dental implant surface and the human bone. Mater (Basel). 2017;10:E1438.
28. Lim JY, Donahue HJ. Cell sensing and response to micro- and nanostructured surfaces produced by chemical and topographic patterning. Tissue Eng. 2007;13:1879–1891.
29. Nouri A, Hodgson PD, Wen C. Biomimetic porous titanium scaffolds for orthopaedic and dental applications. In: Mukherjee A, ed. Biomimetics, Learning from nature. Croatia: InTechOpen. 2010; p. 415–450.
30. Gligor I, Soritau O, Todea M, Berce C, Vulpoi A, Marcu T et al. Porous c.p. titanium using dextrin as space holder for endosseous implants. Part Sci Technol. 2012;31:357–365.
31. Hrabe NW, Heinl P, Bordia RK, Korner C, Fernandes RJ. Maintenance of a bone collagen phenotype by osteoblast-like cells in 3D periodic porous titanium (Ti-6Al-4 V) structures fabricated by selective electron beam melting. Connect Tissue Res. 2013;54:351–360.
32. de Oliveira MV, Moreira AC, Pereira LC.Porosity characterization of sintered titanium scaffolds for surgical implants. Mater Sci Forum. 2008;591-593:36–41.